2-7-2009

# Imaging Radiation Pneumonitis in a Rat Model of a Radiological Terrorism Incident

Robert C. Molthen
*Marquette University*

QingPing Wu
*Medical College of Wisconsin*

Gary S. Krenz
*Marquette University*, gary.krenz@marquette.edu

Meetha Medhora
*Medical College of Wisconsin*

Elizabeth R. Jacobs
*Medical College of Wisconsin*

*See next page for additional authors*

# Imaging Radiation Pneumonitis in a Rat Model of a Radiological Terrorism Incident

Robert Molthen[1,2,3], QingPing Wu[1], Gary Krenz[1,2,3,4], Meetha Medhora[1], Elizabeth Jacobs[1], and John E. Moulder[5]

[1] Division of Pulmonary and Critical Care, Department of Medicine, Medical College of Wisconsin, Milwaukee, WI, USA 53226
[2] Department of Veteran's Affairs, Zablocki VA Medical Center, Milwaukee, WI, USA 53295
[3] Department of Biomedical Engineering, Marquette University, Milwaukee, WI, USA 53201
[4] Department of Math, Statistics and Computer Science, Marquette University, Milwaukee, WI 53201
[5] Department of Radiation Oncology, Medical College of Wisconsin, Milwaukee, WI, USA 53226

## ABSTRACT

We have developed a rat model of single, sub-lethal thoracic irradiation. Our irradiation protocol is considered representative of exposures near the detonation site of a dirty bomb or small nuclear device. The model is being used to investigate techniques for identifying, triaging and treating possible victims. In addition to physiological markers of right ventricular hypertrophy, pulmonary vascular resistance, and arterial distensibility, we present two methods for quantifying microvascular density. We used methods including microfocal X-ray imaging to investigate changes in lung structure/function resulting from radiation exposure. Radiation pneumonitis is a complication in subjects receiving thoracic irradiation. A radiographic hallmark of acute radiation pneumonitis is a diffuse infiltrate corresponding to the radiation treatment field. We describe two methods for quantifying small artery dropout that occurs in the model at the same time-period. Rats were examined 3-days, 2-weeks, 1-month (m), 2-m, 5-m, and 12-m post-irradiation and compared with aged-matched controls. Right ventricular hypertrophy and increases in pulmonary vascular resistance were present during the pneumonitis phase. Vascular injury was dependent on dose and post-irradiation duration. Rats irradiated with 5 Gy had few detectable changes, whereas 10 Gy resulted in a significant decrease in both microvascular density and arterial distensibility around 2-m, the decrease in each lessening, but extending through 12-m. In conclusion, rats irradiated with a 10 Gy dose had changes in vascular structure concurrent with the onset of radiation pneumonitis that were detectable with our imaging techniques and these structural changes persist after resolution of the pneumonitis.

**Keywords:** pneumonitis, radiation, rat, X-ray, microfocal, imaging, vascular density, arteriogram, terrorism

## 1. INTRODUCTION

Currently there are limited radioprotectors, therapeutics, and prophylactic treatments that are safe and effective to prepare patients or personnel before they are knowingly exposed to radiation, and there are no 'retrospective' agents approved for use to mitigate injury from radiation exposure after the fact. The threat of nuclear or radiological terrorism along with the broadening role of radiation therapy in oncology establishes imperatives to develop countermeasures to quantify exposure, mitigate effects before injury becomes evident, and treat injuries as symptoms ensue. Ideally, radioprotectors and therapeutics should be safe in multiple doses for all populations, chemically stable, easily

Medical Imaging 2009: Biomedical Applications in Molecular, Structural, and Functional Imaging, edited by Xiaoping P. Hu, Anne V. Clough, Proc. of SPIE Vol. 7262, 72620X · © 2009 SPIE · CCC code: 1605-7422/09/$18 · doi: 10.1117/12.810935

administered, and rapidly effective. In addition, the new preparedness and response paradigm, eliminates agents that work only when given before radiation exposure and desperately requires methods to triage mass casualties and perform accurate biodosimetry in the scenario of radiological dispersal to reduce overwhelming medical facilities by eliminate concerned 'victims' who have not actually been exposed to biologically significant radiation[1, 2].

The lung is relatively sensitive to radiation-induced injury. In the scenario of radiological (nuclear) terrorism, it is likely that radioactive compounds would be aerosolized or at least airborne and make the lung tissue a likely accumulator/target[3]. Victims that receive significant radiation exposure and survive acute radiation syndrome, infection, hemomatopoietic and GI injury, would need to be managed through delayed complications, including interstitial pneumonitis, chronic renal failure, and developmental abnormalities. A large percentage of people receiving radiation to the chest will develop either symptomatic injury or asymptomatic reduction of pulmonary function. The typical injury occurring within 3-6 months of irradiation is manifested as pneumonitis[4], which presents as a cough, shortness of breath, and occasionally, fever. Pneumonitis is characterized histologically by loss of epithelial cells, airspace and interstitial edema, and inflammatory infiltrate. Later phase injury appearing 6-12 months post-irradiation manifests as interstitial fibrosis, focal scarring, and loss of alveoli that results in a progressive shortness of breath.

This study is part of the Center for Radiation Injury Intervention (www.centrii.org). CENTRII is one of five Centers for Medical Countermeasures Against Radiation (CMCR's) established by an RFA from NIH/NCI. The center is developing animal models of irradiation injury and methods to triage, mitigate and treat it[5]. Our group concentrates it efforts on understanding and treating radiation-induced lung injury. This study we use a rodent (rat) model of penetrating radiation injury confined to the thorax towards the goal of developing strategies to detect, quantify, and mitigate pneumonitis and pulmonary fibrosis. Our focus in this paper is the use of microfocal X-ray imaging to quantify changes in the pulmonary arterial structure near the acute phase of radiation-induced pnuemonitis.

## 2. METHODOLOGY

### 2.1 Injury model

A Pantak HF320 orthovoltage system (Therapax, Danbury, CT, USA) was used to irradiate the thorax of female WAG/Rij/MCW rats (110-170 gm) with 5Gy (N=24) or 10 Gy (N=104). These doses are significantly lower than used in many previous studies of radiation induced lung injury[6-10]. The rats were placed in a plexiglass holding jig and customized lead shielding was used to limit radiation exposure to the thorax. More details on the irradiation physics and methods are described previously[11, 12]. The absolute dose was measured using a calibrated Farmer-type ionization chamber. The radiation dose was delivered by two equally-weighted lateral beams in order to improve the dose uniformity. The whole lung is in the field, plus the heart and a small amount of the liver. All the studies were done under approval of the Medical College of Wisconsin and Zablocki VA Medical Center IACUC review boards and in compliance with the National Research Council's Guide for the Care and Use of Laboratory Animals. Irradiated rats and their age-matched controls were studied at time points of 3-days, 2-weeks, and 1, 2, 5, and 12-months after irradiation.

### 2.2 Lung preparation, imaging and analysis

Methods and analysis follow those previously described[13]. Briefly, rats were anesthetized with sodium pentobarbital (40mg/kg), heparinized and blood sampled from the right ventricle via midline sternotomy, the trachea and pulmonary artery were cannulated, the heart excised and lungs removed. The heart, the right ventricle was dissected away from the septum and right ventricular hypertrophy was assessed as the ratio of the weight of the right ventricle to that of the left ventricle plus septum (RV/LV+S). The lungs were hung by the cannulae, ventilated, sighed, rinsed of blood, and perfused with a 5% BSA physiological saline solution (Equitech-Bio Inc, Kerrville, Texas, USA).

Ventilation was halted at an airway pressure of 6 mmHg and pulmonary artery pressure was measured at perfusion flow rates of 30, 20, 15, 10, 5, and 0 ml/min to measure pulmonary vascular resistance. For comparison of pressure vs. flow between lungs, flow rates were normalized by total body weight. For imaging the lung placed in a humidified specimen holder, ventilation was again halted at an airway pressure of 6 mmHg. The perfusate was replaced with perfluorooctyl bromide (PFOB, 1-bromo-perfluoro-octane, Crescent Chemical Co. Inc, Islandia NY, USA) for X-ray contrast. PFOB does not pass through the capillary bed, so intravascular pressures can be maintained constant hydrostatically. Vessels were conditioned by cycling the intravascular pressure from 0 to 35 mmHg several times, then intravascular pressure

was set to 30, 21, 12, and 5 mmHg and low- and high-magnification microfocal angiographic imaging performed at each pressure. For CT imaging, the lungs were rotated in the X-ray beam at 1° increments to obtain 360 planar images and the source-to-object distance was approximately 29 cm. Figure 1 shows example low-magnification images from a 0Gy control and a 10Gy irradiated rat lungs 2-m after the start of the protocol. For high-magnification planar images, the source-to-object distance was decreased to approximately 3 cm. Figure 2 shows example high-magnification images in lungs from 0Gy control and 5 and 10Gy irradiated rats, 3-d, 2-wk, 1-m, 2-m, 5-m, and 12-m after the start of the protocol (post-irradiation). In both modes of imaging, source-to-detector distance was 89.0 cm, the source voltage set to 41 kV and source current to 140 μA.

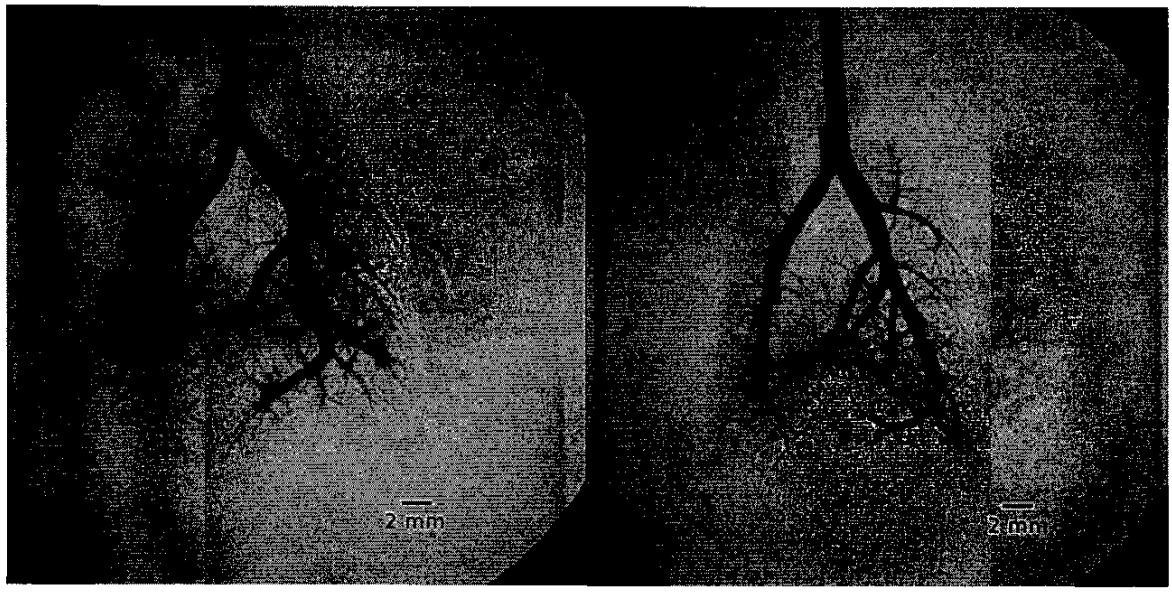


Fig. 1. Example 512x512 pixel, low-magnification planar angiograms in lungs isolated from a 0Gy control (left) and a 10Gy irradiated (right) rat at the 2-month end-point. The arteries are filled with perfluorooctyl bromide at an intravascular pressure of 30 mmHg. Source-to-detector distance = 89.0 cm, source-to-object distance ≅ 29 cm, source voltage = 41 kV, and source current = 140 μA. Lungs are supported by contrast filled plastic cannulae with inner diameter = 1.67 mm. The scale bar in the bottom, right of the images is approximately 2 mm.

The imaging system is composed of a Feinfocus FXE/FXT 100.20 microfocal X-ray source (3 μm effective focal spot), a Thomson TH9438 HX H661 VR24 image intensifier (detector) optically coupled to a Silicon Mountain Design (SMD1M-15) CCD, and a New England Affiliated Technologies (NEAT) specimen micromanipulator stage, all mounted on a precision rail with positional information provided by Mitutoyo linear encoders accurate to 10 μm. The camera was set for 512x512 pixel resolution and data transferred via RS-422 interface to a frame grabber board mounted in a Dell 610 workstation. Each planar projection image was a result of averaging 7 frames on the frame grabber to reduce noise. Image acquisition and positional control were preformed by software written in-house, running under WindowsNT. After preprocessing, that compensates for field distortions and nonuniformities introduced by the imaging chain[14], low-magnification planar images were used to create isotropic CT reconstructions through an implementation of the Feldkamp cone-beam algorithm[15]. The typical isotropic volume was $497^3$ pixels with a pixel size of approximately 70 μm.

### 2.2.1 Arterial distensibility

Arterial distensibility was measured using previously published methods[13]. Briefly, isotropic CT volumes were used to map and measure the main pulmonary trunk at each intravascular pressure. To estimate vessel segment diameter, the grayscale image data was fit, using an unconstrained multivariable non-linear optimization function 'fminunc' in the Matlab (MathWorks, Natick, MA) optimization toolbox. An estimate of arterial distensibility was then made by fitting

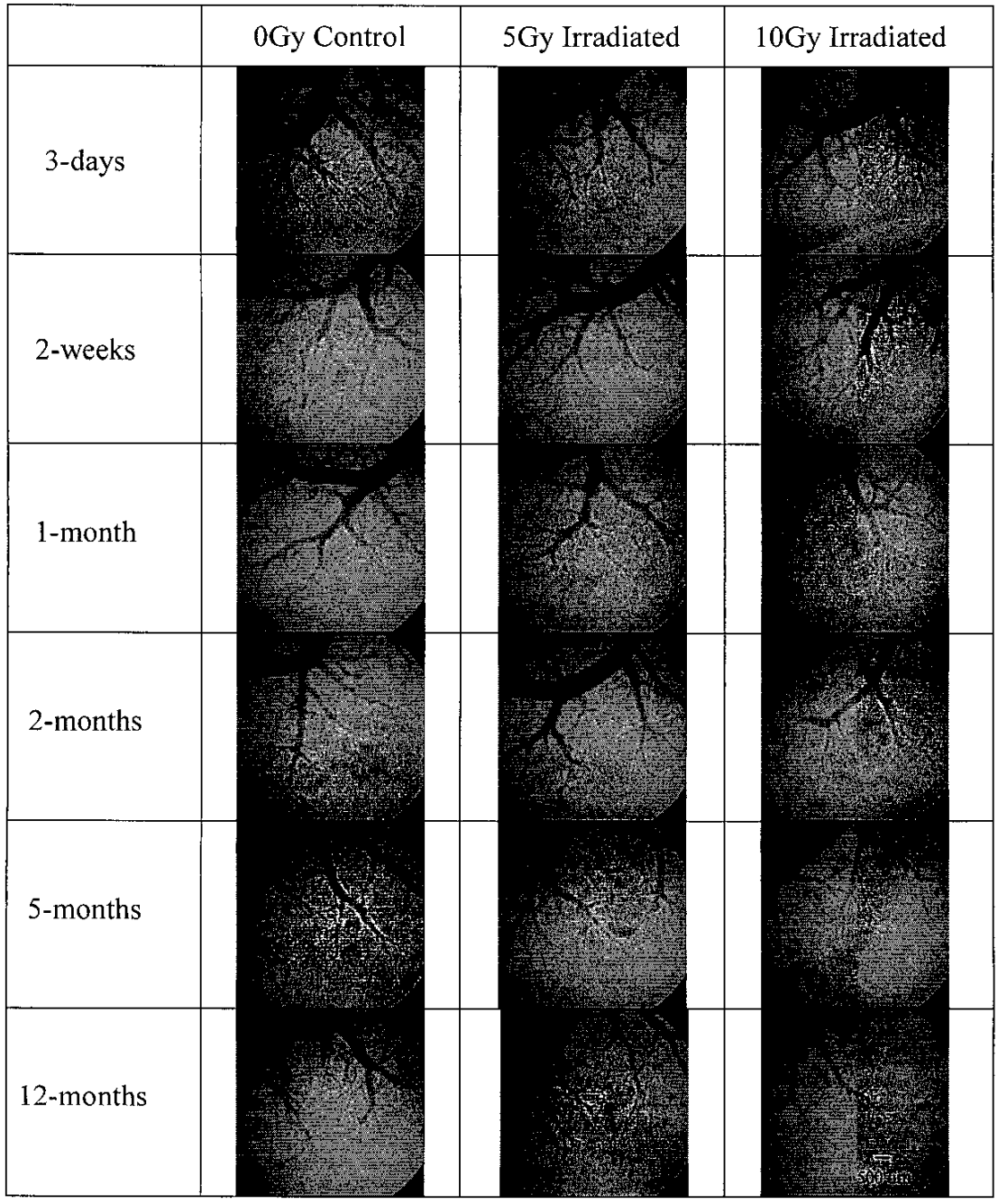


Fig. 2. Example 512x512 pixel high-magnification planar angiograms of the lower, right lung isolated from 0Gy control (2nd column), 5Gy irradiated (3rd column) and 10Gy irradiated (4th column) rats. The arteries are filled with PFOB at an intravascular pressure of 30 mmHg. Source-to-detector distance = 89.0 cm, source-to-object distance ≅ 3 cm, source voltage = 41 kV, and source current = 140 μA. Text in the 1st column indicates time of end-point study. The scale bar in the bottom, right image indicates approximately 500 μm. Pixel size ≅15 μm.

the diameter vs. distance from the main trunk inlet vs. intravascular pressure to a morphometric model of the pulmonary arterial tree, also performed using the Matlab fminunc function.

### 2.2.2 Microvascular density

Differences in microvascular density could be visualized in high-magnification planar arteriograms. Rats receiving radiation had perceptible decreases in microvascular density. In this study, we investigated 2 image processing methods to quantitatively estimate a microvascular density index (MVDi) from high-magnification planar angiograms of the right, lower lung lobe. Matlab code was developed to provide a user interface for the analysis of planar images. Lungs were analyzed at an intravascular pressure of 30 mmHg, at which changes in microvascular denisty were best visualized. The first method used a 'large' 200x100 pixel primary region of interest (ROI) and a second smaller 25x25 pixel ROI subregion within the first, both designated by an operator. The second method only requires that the initial 200x100 pixel ROI is designated. For either method, the planar images were first normalized by dividing by their respective flood field image. The margin of the lung (the lower basal edge of the right lung) was included in the imaged field of view, see Figure 2 & 3. The operator identifies two points, at least 200 pixels apart, along the edge of the lung, see Figure 3 A & B. The code uses the coordinates of the two locations along the lung edge identified to create a rectangular ROI 200 pixels (3 mm) long extending 100 pixels (1.5 mm) into the lung parenchyma, see Figure 3 C & D. Both methods determine a grayscale value to be used as a threshold to segment the larger ROI into pixels categorized as 'vessel' and pixels categorized as 'non-vessel'.

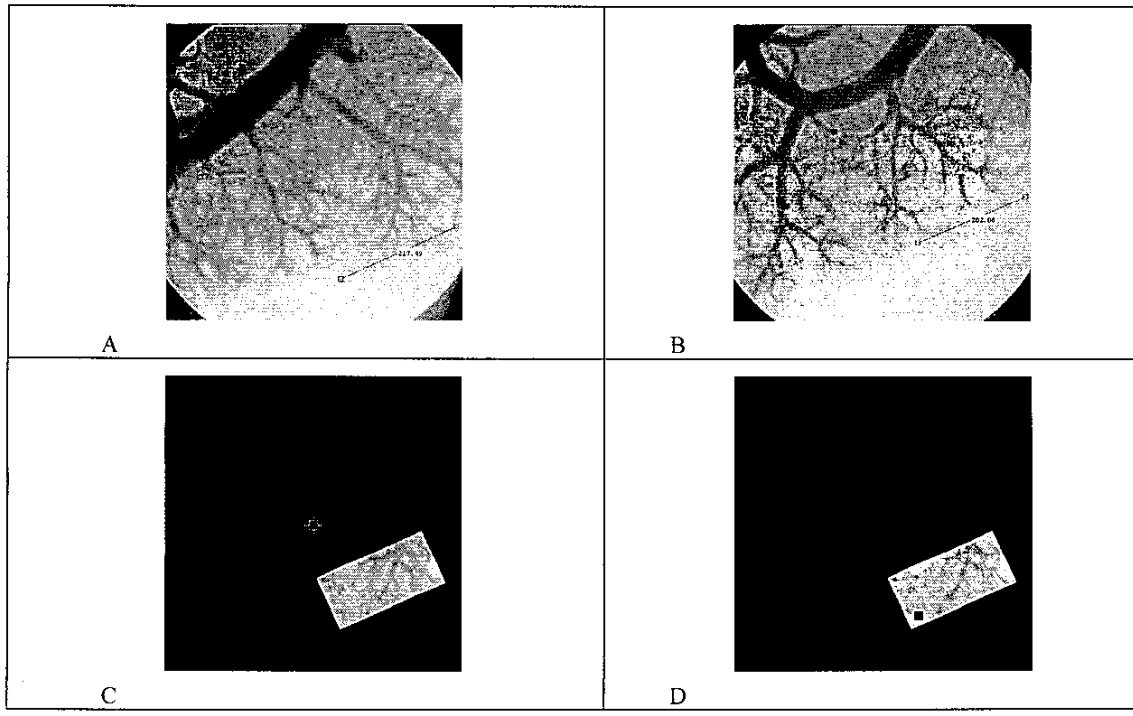


Fig. 3. Example high-magnification planar angiograms of the lower, right lung isolated from a 0Gy control (A) and a 10Gy irradiated rat (B) at the 2-month end-point. Dumb-bell shaped line at edge of lungs represents the graphical user interface tool used by operator to identify edge of lung and subsequent ROI. (C), a 200x100 pixel primary ROI from a lung region in A indicates the data that is used for analysis. (D), a small black square indicates background ROI chosen to be void of visually detectable vessels within the original larger ROI.

### 2.2.2.1 Background Minimum Method

The Background Minimum (BM) method determines a vascular threshold employing two operator-selected ROIs: The primary ROI is selected along the base of the lung, while a second ROI is selected from within the primary ROI at a location that is free of any discernable vessels, see Figure 3D. This second ROI represents the background lung parenchyma and should only contain vessels that are either too small to be resolved by the imaging system or are not filled with PFOB. The threshold in the BM method is determined as the minimum grayscale value in the background ROI. This minimum value corresponds to the darkest pixel in the background or the 'most vessel-like' pixel available in the background ROI. Using this threshold, the data in the large ROI was converted into a binary image (grayscale value <= threshold corresponds to a vessel (black), otherwise the data are non-vessel (white)), see Figure 5 A & B. The binary ROI was then converted to a quantitative MVDi by dividing the number of pixels that are designated as 'vessel' by the total number of pixels in the ROI.

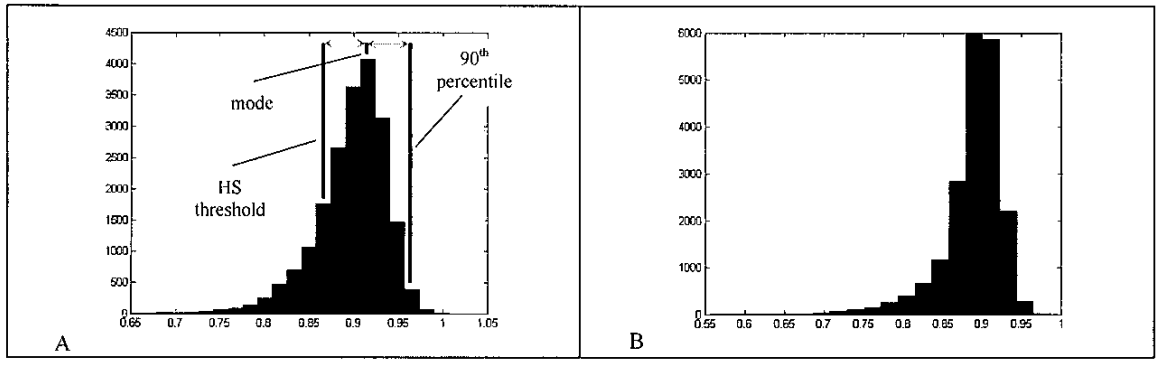


Fig. 4. Example histogram of grayscale data from primary ROI in a control 0Gy rat lung (A) and an irradiated 10Gy rat lung (B) studied at the 2-month end-point. Three thick vertical black lines in (A) represent the Histogram Symmetry (HS) threshold, the grayscale mode, and the 90th percentile. Two thin horizontal gray lines with arrowheads indicate the 'scale' used to determine the HS threshold.

### 2.2.2.2 Histogram Symmetry Method

In the Histogram Symmetry (HS) method, the operator selects a ROI at the edge of the lung in the high-magnification planar image similar to the BM method, see Figure 3C. For comparison in this study, the same ROI used for the BM method was used for the HS method. A histogram of the grayscale data within the ROI was assembled using 20 bins, see Figure 4 A & B. The HS grayscale threshold was then determined as the mode of the histogram minus the difference between the grayscale value at the 90th percentile and the mode. Conceptually, the threshold calculated by this criterion can be thought of as determining the variation in the histogram from a [symmetric] Gaussian distribution. In the absence of vessels, a grayscale histogram of a background ROI should approximate a Gaussian distribution. Since pixels resulting from transmission of the X-rays through vessels likely have grayscale values below the histogram mode, we assume the portion of the histogram above the mode will follow a Gaussian distribution. The difference in the grayscale mode and that at a chosen percentile can then be used as a 'scale', see Figure 4A, and subtracted from the mode to provide a threshold value below which pixels will likely contain information about 'vessels'. Our choice for this study was the 90th percentile, determined through trial and error comparing resulting binary images to grayscale images of the underlying vascular structure. The threshold determined using this criterion was then used to convert the ROI into a binary image, see Figure 5 C & D, and again the binary ROI was transformed into MVDi by dividing the number of pixels that were designated as 'vessel' by the total number of pixels in the ROI.

### 2.3 Statistical analysis

Data on parameters was calculated and presented as mean ± standard error of the mean. All statistical comparisons were performed in SigmaStat 3.0 (SPSS, Chicago, IL) using an unpaired t-test ($P \leq 0.025$). If the normality test failed, a Mann-Whitney Rank Sum test was run to confirm significance.

## 3. RESULTS

Lungs of animals irradiated with a single thoracic dose of 5Gy had remarkably few qualitative or quantitative changes as detected by our methods, although there was a marginal, but significant, increase in right ventricular hypertrophy at 5-m and indication there may be a microvascular density decrease at later end-points. In contrast, animals that receive a 10Gy exposure had significant morbidity and pulmonary vascular changes. Compared to age-matched controls, animals

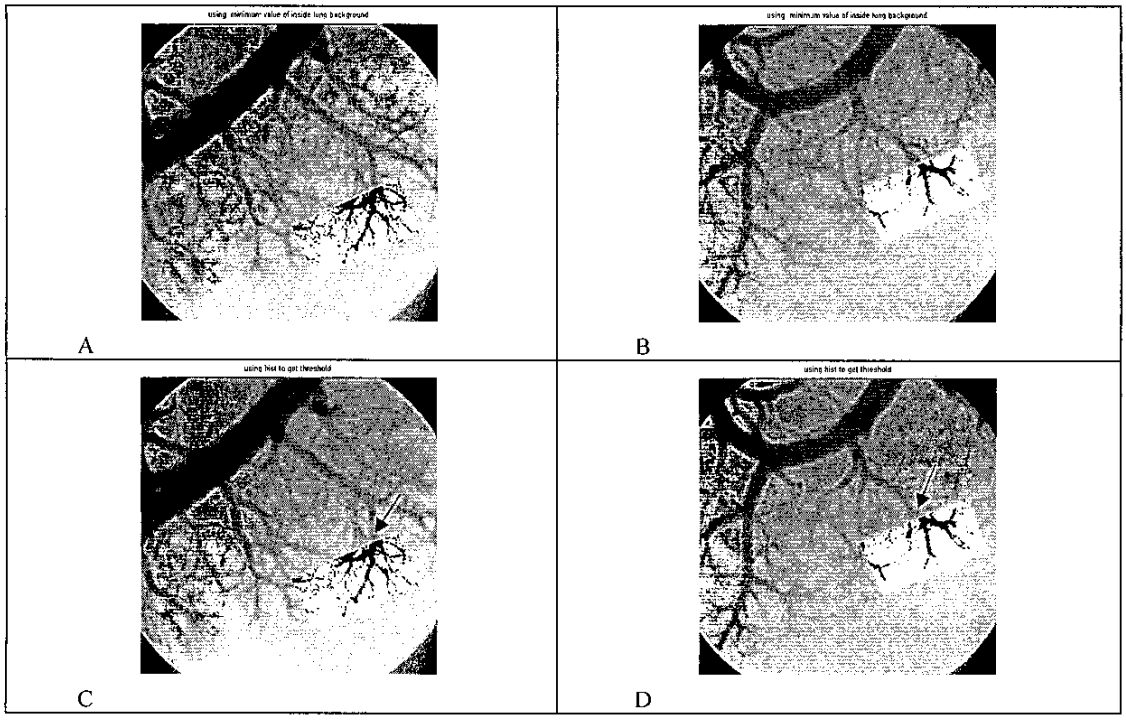


Fig. 5. Example high-magnification planar angiogram in a lung isolated from a 0Gy control (left side, A & C) and a 10Gy irradiated (right side, B & D) rat at the 2-month end-point, same lungs as shown in Figure 3. The Background Minimum (BM) method A & B and the Histogram Symmetry (HS) method C & D were used to determine an appropriate threshold to create a binary image (black=vessel and white=non-vessel) overlaid on the ROI. For scale reference, the vessels entering into the ROI (arrow) are approximately 200 μm in diameter.

receiving a 10Gy dose had significantly lower body weight at 2-m and 12-m, significantly increased pulmonary vascular resistance at 1-m, 2-m, and 5-m, significantly increased right ventricular hypertrophy at 2-m, and a dry lung weight significantly increased at 1-m to 12-m. In addition, pulmonary artery distensibility was significantly lower than age-matched controls starting at 2-m and the arteries remained significantly stiffer to at least 12-m. A number of independent observers visualized a decrease in small vessel density in low- and high-magnification planar angiograms of irradiated rats. We developed 2 independent methods for estimating and quantifying a microvascular density index (MVDi) from angiograms of the isolated rat lung. The BM method detected a significant decrease in the MVDi of 10Gy exposed rats at 2-m through 12-m, see Figure 6A. The HS method detected this decrease in microvascular density in the same time-period, and additionally, a significant MVDi decrease in lungs at the 1-m end-point, see Figure 6B. There was less visually identifiable evidence of decreased microvascular density in rats irradiated with 5Gy. The BM and HS methods were used to analyze data at 2-m, 5-m, and 12-m after irradiation with a 5Gy dose. The BM analysis results indicate a significant decrease in MVDi at 12-m, see Figure 7A. However, the HS analysis resulted in no significant difference in the MVDi at this time-point, see Figure 7B.

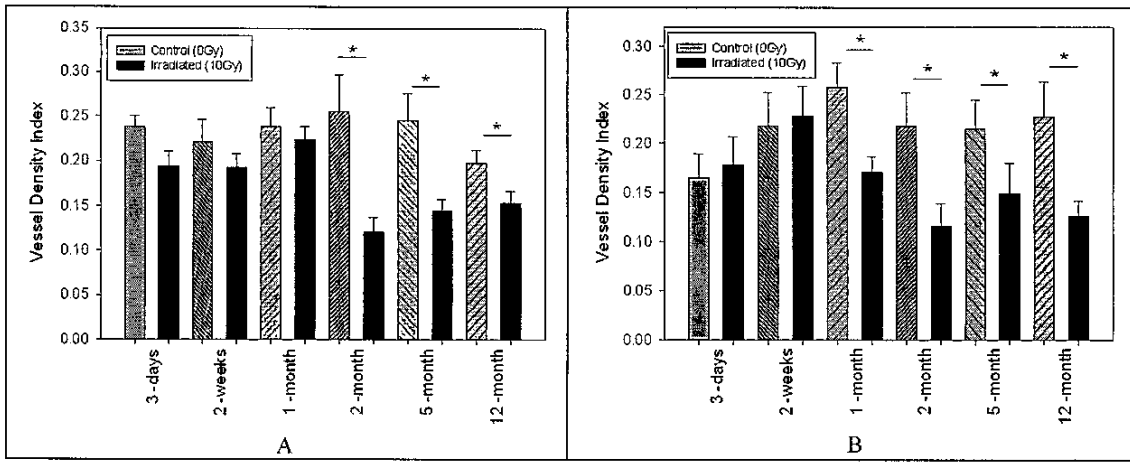


Fig. 6. Microvascular density index (MVDi) determined using the Background Minimum (BM) method (A) and the Histogram Symmetry (HS) method (B) in lungs of 0Gy control and 10Gy irradiated rats at end-points of 3-days, 2-weeks, 1-month, 2-months, 5-months, and 12-months. N = 8-11 rats in each group. Mean ± standard error.

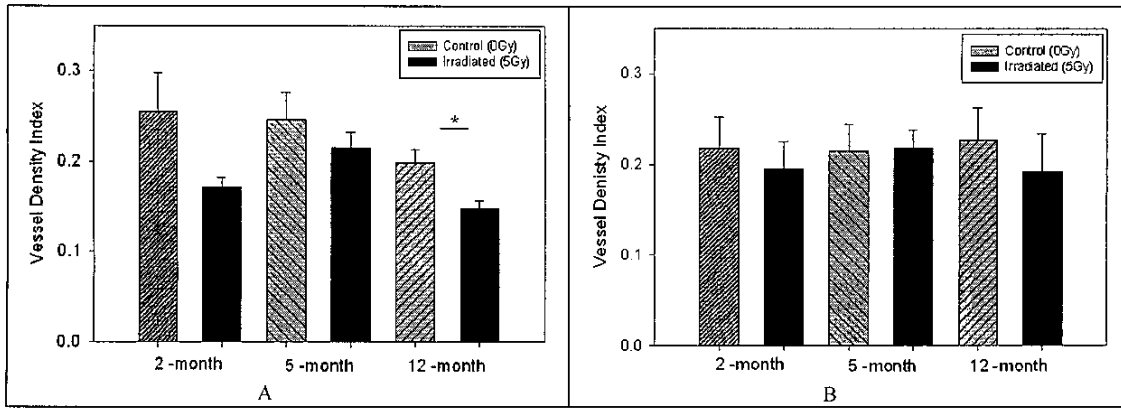


Fig. 7. Microvascular density index (MVDi) determined using the Background Minimum (BM) method (A) and the Histogram Symmetry (HS) method (B) in lungs of 0Gy control and 5Gy irradiated rats (B) at end-points of 2-months, 5-months, and 12-months. N = 7-9 rats in each group. Mean ± standard error.

## 4. CONCLUSIONS / DISCUSSION

In this rat model of radiation-induced lung injury, a single 10Gy dose, limited to the thorax, caused significant pulmonary vascular remodeling[11]. Pneumonitis was evident in the animals at 1-to-2-m post-irradiation, accompanied by increased pulmonary vascular resistance and right ventricular hypertrophy, both subsequently resolving. Using microfocal X-ray imaging, we detected a decrease in arterial distensibility and vascular drop-out, at the same time. Vascular drop-out and decreased distensibility partially resolved, but persisted to 12-m. The pneumonitis was not seen in the rats at the 5-m and 12-m end-point. Many of these finding are consistent with previous studies of radiation injury in the rat lung[16]. The classic radiographic presentation of radiation-therapy induced pneumonitis, with regional or patchy consolidation, was not seen. This is likely do to the relatively low-dose exposure field being nearly uniform across the rat thorax, which is in contrast to what we have found with regional lung exposure in a similar rat model of irradiation[17]. The perfluorooctyl bromide (PFOB) used as the vascular contrast agent does not pass freely through the

capillary bed. The luminal diameter at which the PFOB gets restricted depends on local surface tension properties, vascular structure, and the intravascular pressure. Therefore, the apparent vessel drop-out or decrease in microvascular density could be caused by 1) an actual reduction of the number of vessels present, 2) decreased filling because the luminal space has decreased, or 3) decreased filling because vessel distensibility has decreased. Significant perivascular edema existed in the lungs at this end-point[11]. Decrease in the perivascular space is a likely reason for at least some of the vessel drop-out at 2-m. The sudden decrease in arterial distensibility measured at 2-m compared to 1-m[12], could also be explained, at least in part, by the limited perivascular space. At the 12-m end-point, decreased microvascular density detected through imaging is more likely a result of the luminal loss due to the increased vessel wall thickening seen at this time-point, since perivascular edema is greatly reduced at 12-m. The decreased arterial distensibilty measured at this end-point is likely also a result of the increase in wall muscularization and increased extracellular matrix components, which limit luminal filling at equivalent intravascular pressures.

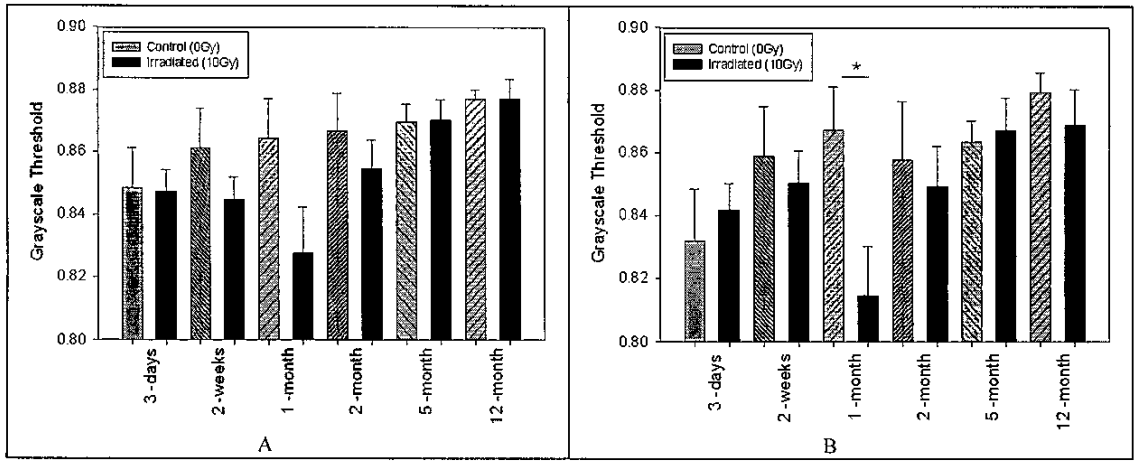


Fig. 8. Grayscale threshold determined using the Background Minimum (BM) method (A) and the Histogram Symmetry (HS) method (B) in lungs of 0Gy control and 10Gy irradiated rats (B) at end-points of 3-days, 2-weeks, 1-month, 2-months, 5-months, and 12-months. N = 8-11 rats in each group. Mean ± standard error.

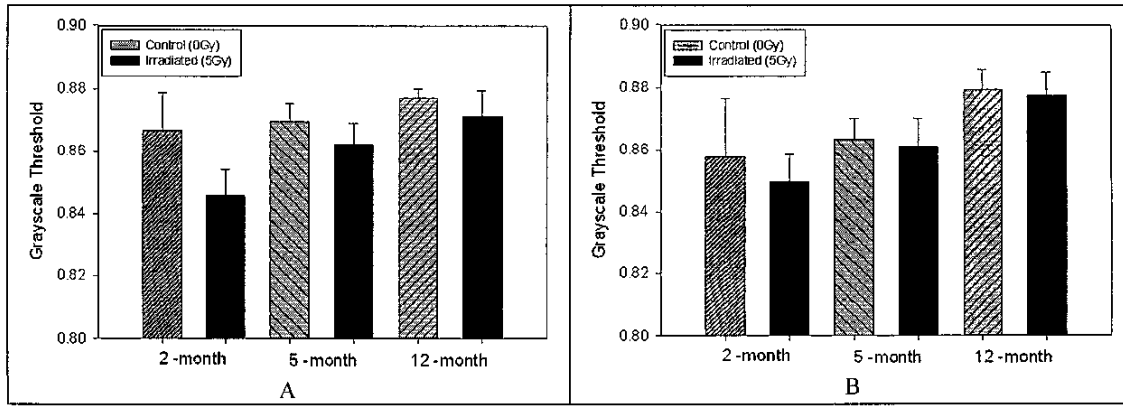


Fig. 9. Grayscale threshold determined using the Background Minimum (BM) method (A) and the Histogram Symmetry (HS) method (B) in lungs of 0Gy control and 5Gy irradiated rats (B) at end-points of 2-months, 5-months, and 12-months. N = 7-9 rats in each group. Mean ± standard error.

Interestingly, besides increased right ventricular hypertrophy at 5-m in the rats irradiated with 5Gy, there was very little evidence of injury. It was not easy to identify systematic differences in lung microvascular density by visual observation of the high-magnification planar images in rats irradiated with 5Gy compared to their age-matched controls. However, there were indications of decreased microvascular density at later end-points. Although MVDi followed a similar trend in the 5Gy irradiated rats, results from applying the BM and HS methods were inconsistent. At the 12-m end-point, the BM method resulted in a significant difference in MVDi, see Figure 7A, whereas the HS method showed no differences, see Figure 7B. Since the BM method relies on the operators choice of positioning for the background ROI, it is sensitive to finding an ROI that is free of visible vessels. Identifying such a region can be a difficult task in both 0Gy control lungs as well as many of the lungs irradiated with 5Gy. A systematic and rigorous analysis to determine a receiver operator characteristic (ROC) curve was not implemented, however, future ROC analysis and studies to analyze the remaining 5Gy data is warranted.

Although there may be slight differences in the thickness of the lungs at the location of the ROIs that were chosen for analysis, 'anchoring' the border of the ROI to the edge of the lung and choosing a similar location in each lung minimizes any variations in thickness. It is reasonable to assume that the difference in the number of vessels seen and the MVDi quantified by both methods for control compared to irradiated rats, was not due to any bias in the thickness of the lung samples. The assumption is supported by the result that the threshold determined, by both the BM and HS methods, was lower for irradiated animals compared to controls, see Figures 8 & 9.

It is also apparent from Figures 8 & 9 that a strategy of applying a simple global threshold does not work for identifying vessels within this data. There tended to be a general increase in the grayscale threshold required for vessel detection from early end-points to later ones. This trend is likely a reflection of a larger airspace-to-tissue ratio present as the lung matures[18]. There is also a dip in the grayscale threshold near the period where the pneumonitis is present, as seen in Figure 8, which likely reflects the inflammation present in the lungs during this period.

The current study used 20 bins in the histogram of the HS method. This results in a fairly coarse discretization of the grayscale values contained in the ROI. Use of a larger number of bins would have likely resulted in a finer discrimination between 'vessel' and 'non-vessel', since the range of grayscale values that fall into the $90^{th}$ percentile bin would be smaller. The sensitivity of the HS method to the number of bins in the histogram and the percentile criterion and the sensitivity of both BM and HS methods to variables such as the size, shape, location, and number of ROIs used to estimate MVDi also warrants further investigation.

In conclusion, with this irradiation protocol, the entire thorax receives a uniform dose and classic radiographic evidence of patchy radiation pneumonitis was not present. Only a slight and mostly homogeneous increase in lung radiopacity was present concurrent with the pneumonitis. The decrease in the grayscale threshold, determined by both BM and HS methods at approximately 2-m in rats irradiated with a 10Gy dose, signifies this increase in lung density, see Figure 8. Rats that received a 10 Gy dose had physiological differences as early as 1-month post-irradiation compared to their age-matched controls. Rats irradiated with 10Gy had changes in vascular structure concurrent with the onset of radiation pneumonitis, detectable with our imaging techniques. Rats that received a 5Gy dose had little measurable injury at any time-point. We also found that changes in vascular structure persist after resolution of the pneumonitis and that both BM and HS methods appears to confirm the visual appearance of the underlying microvascular bed.

## ACKNOWLEDGEMENTS

The authors would like to acknowledge funding from National Institute of Health, National Cancer Institute, U19 AI067734-01, and the Veterans Administration. The authors would also like to thank Brian Fish, Ying Gao, Stephanie Gruenloh, Swarajit Ghosh, Ying Dena Hall, Tarrant Csida, Mary Lou Mader, and Yvonne Morauski for help with the animals, administration, studies, and their dedication to the goals of the Center for Radiation Injury Intervention.

## REFERENCES

[1] J. E. Moulder, "Post-irradiation approaches to treatment of radiation injuries in the context of radiological terrorism and radiation accidents: a review," Int J Radiat Biol, 80(1), 3-10 (2004).

[2] H. B. Stone, J. E. Moulder, C. N. Coleman *et al.*, "Models for evaluating agents intended for the prophylaxis, mitigation and treatment of radiation injuries. Report of an NCI Workshop, December 3-4, 2003," Radiat Res, 162(6), 711-28 (2004).

[3] A. J. Gonzalez, "Lauriston S. Taylor Lecture: Radiation protection in the aftermath of a terrorist attack involving exposure to ionizing radiation," Health Phys, 89(5), 418-46 (2005).

[4] N. J. Gross, "The pathogenesis of radiation-induced lung damage," Lung, 159(3), 115-25 (1981).

[5] A. D. Augustine, T. Gondre-Lewis, W. McBride *et al.*, "Animal models for radiation injury, protection and therapy," Radiat Res, 164(1), 100-9 (2005).

[6] A. Molteni, J. E. Moulder, E. F. Cohen *et al.*, "Control of radiation-induced pneumopathy and lung fibrosis by angiotensin-converting enzyme inhibitors and an angiotensin II type 1 receptor blocker," Int J Radiat Biol, 76(4), 523-32 (2000).

[7] W. F. Ward, N. H. Solliday, A. Molteni *et al.*, "Radiation injury in rat lung. II. Angiotensin-converting enzyme activity," Radiat Res, 96(2), 294-300 (1983).

[8] Z. Vujaskovic, M. S. Anscher, Q. F. Feng *et al.*, "Radiation-induced hypoxia may perpetuate late normal tissue injury," Int J Radiat Oncol Biol Phys, 50(4), 851-5 (2001).

[9] L. Kwock, W. C. Davenport, R. L. Clark *et al.*, "The effects of ionizing radiation on the pulmonary vasculature of intact rats and isolated pulmonary endothelium," Radiat Res, 111(2), 276-91 (1987).

[10] M. M. Graham, M. L. Evans, D. D. Dahlen *et al.*, "Pharmacological alteration of the lung vascular response to radiation," Int J Radiat Oncol Biol Phys, 19(2), 329-39 (1990).

[11] R. Zhang, S. N. Ghosh, D. Zhu *et al.*, "Structural and functional alterations in the rat lung following whole thoracic irradiation with moderate doses: injury and recovery," Int J Radiat Biol, 84(6), 487-97 (2008).

[12] W. Q. Ghosh S.N., Mäder M., Fish B.L., Moulder J.E., Jacobs E.R., Medhora M., Molthen R.C., "Vascular Injury Following Whole Thoracic X-ray Irradiation in the Rat," International Journal of Radiation Oncology, Biology, Physics, 10.1016/j.ijrobp.2009.01.006 (in press).

[13] R. C. Molthen, K. L. Karau, and C. A. Dawson, "Quantitative models of the rat pulmonary arterial tree morphometry applied to hypoxia-induced arterial remodeling," J Appl Physiol, 97(6), 2372-84; discussion 2354 (2004).

[14] K. L. Karau, R. H. Johnson, R. C. Molthen *et al.*, "Microfocal X-ray CT imaging and pulmonary arterial distensibility in excised rat lungs," Am J Physiol Heart Circ Physiol, 281(3), H1447-57 (2001).

[15] L. A. Feldkamp, L. C. DAVIS, and J. W. KRESS, "Practical cone-beam algorithm," Journal of the Optical Society of America A, 1(6), 612-619 (1984).

[16] L. M. Peterson, M. L. Evans, M. M. Graham *et al.*, "Vascular response to radiation injury in the rat lung," Radiat Res, 129(2), 139-48 (1992).

[17] V. A. Semenenko, R. C. Molthen, C. Li *et al.*, "Irradiation of varying volumes of rat lung to same mean lung dose: a little to a lot or a lot to a little?," Int J Radiat Oncol Biol Phys, 71(3), 838-47 (2008).

[18] H. G. Ringertz, R. C. Brasch, C. A. Gooding *et al.*, "Quantitative density-time measurements in the lungs of children with suspected airway obstruction using ultrafast CT," Pediatr Radiol, 19(6-7), 366-70 (1989).